

# Structural behavior of arch dams considering experimentally validated prototype model using similitude and scaling laws

Ahmet Can Altunışık\*, Ebru Kalkan<sup>a</sup> and Hasan B. Başağa<sup>b</sup>

Department of Civil Engineering, Karadeniz Technical University, Trabzon, Turkey

(Received December 18, 2017, Revised May 15, 2018, Accepted May 17, 2018)

**Abstract.** As one of the most important engineering structures, arch dams are huge constructions built with human hands and have strategical importance. Because of the fact that long construction duration, water supply, financial reasons, major loss of life and material since failure etc., the design of arch dams is very important problem and should be done by expert engineers to determine the structural behavior more accurately. Finite element analyses and non-destructive experimental measurements can be used to investigate the structural response, but there are some difficulties such as spending a long time while modelling, analysis and in-situ testing. Therefore, it is more useful to conduct the research on the laboratory conditions and to transform the obtained results into real constructions. Within the scope of this study, it is aimed to determine the structural behavior of arch dams considering experimentally validated prototype laboratory model using similitude and scaling laws. Type-1 arch dam, which is one of five arch dam types suggested at the “Arch Dams” Symposium in England in 1968 is selected as reference prototype model. The dam is built considering dam-reservoir-foundation interaction and ambient vibration tests are performed to validate the finite element results such as dynamic characteristics, displacements, principal stresses and strains. These results are considered as reference parameters and used to determine the real arch dam response with different scales factors such as 335, 400, 416.67 and 450. These values are selected by considering previously examined dam projects. Arch heights are calculated as 201 m, 240 m, 250 m and 270 m, respectively. The structural response is investigated between the model and prototype by using similarity requirements, field equations, scaling laws etc. To validate these results, finite element models are enlarged in the same scales and analyses are repeated to obtain the dynamic characteristics, displacements, principal stresses and strains. At the end of the study, it is seen that there is a good agreement between all results obtained by similarity requirements with scaling laws and enlarged finite element models.

**Keywords:** arch dam; finite element analyses; scaling laws; similarity requirements

## 1. Introduction

Arch dams are curved in plan, with its convexity towards the upstream side. They are quite suitable for narrow canyons and transfer the water pressure and all forces due to the abutments by arch geometry. The sections of an arch dam are similar to gravity dams but the sections are comparatively thinner. Classification of an arch dam depends on its angle, radius and curvature. There are four types of arch dams such as constant radius, variable radius, constant angle and, double curvature. Since they are thinner and more slender than any other dam types, they require much less construction material, making them economical and practical in remote areas. Due to important curvature of the cantilevers, the low mean thickness of the dam and the length of the arches, the vibration characteristics can be extracted and evaluated more clearly for structural condition assessment.

Arch dams can be exposed to many different loads such as earthquake, blast, wind, ice, and water pressure which may cause deterioration and loss of structural integrity. These loads may have severe economic consequence and, more importantly, may present a serious risk to public safety. So, the structural behavior of arch dams should be monitored and/or controlled at regular intervals during their service life. This is of vital importance, especially before and after the earthquakes. Because earthquake may increase possibility of a dam's damage and ensuing failure. Therefore, structural performance should be determined for the safety assessment of arch dam.

There are many studies in the literature about the determination of structural response of arch dam using finite element analyses (Luo *et al.* 2016, Kalateh and Koosheh 2017, Khiavi 2017, Lokke and Chopra 2017). Also, few studies can be available about the experimental investigation and in-situ testing (Chen *et al.* 2015, Altunışık *et al.* 2016, Wang *et al.* 2016, Huang and Zhu 2017, Zhongzhi *et al.* 2017). But, there is not enough research about the using of prototype structural outputs to evaluate and transform them to the scaled real structures using similarity requirements, field equations, scaling laws. Zhou *et al.* (2000) conducted to experimental works by producing scaled models in order to investigate the cracks that will occur due to earthquake motions in the arch dam designed

\*Corresponding author, Professor  
E-mail: [ahmetcan8284@hotmail.com](mailto:ahmetcan8284@hotmail.com)

<sup>a</sup>Ph.D. Student  
E-mail: [ebrukalkan@ktu.edu.tr](mailto:ebrukalkan@ktu.edu.tr)

<sup>b</sup>Assistant Professor  
E-mail: [hasanbb@ktu.edu.tr](mailto:hasanbb@ktu.edu.tr)

as far as of the earthquake acceleration which the possibility to be exceeded in 500 years have 10%. Oliveira and Faria (2006) aimed to determine the damage levels for arch dams using small scaled models. For this purpose, 1/250 scaled models of the Alqueva and Alto Lindoso Arch Dam having 96m and 110m height are built in the laboratory. Wang and Li (2006) investigated to the earthquake behavior of a dam that have arch height of 278 m and crest length of 612.5 m in China by constructing 1/300 scaled model in laboratory conditions including dam-reservoir-foundation interaction. Wang and He (2007) studied about the crack effect in natural frequencies with experimental studies on large scaled models. The experimental study is conducted on laboratory dam model by Wang and Li (2007) in order to evaluate the earthquake response of Xiao Wan Arch Dam which has 292m height in China. Sevim *et al.* (2011, 2012, 2013, 2014) carried out the non-destructive experimental measurements on scaled Type-1 arch dam model using ambient vibration tests to extract the dynamic characteristics, to investigate the reservoir length and height effect, to present the crack distribution on dam body and evaluate the construction stage analyses. Finally, it is worth noting the work done by Altunışık *et al.* (2015, 2017) on FRP composite effect on the structural response of arch dam model.

Beside these studies, many studies exist about the using of similitude and scaling laws for different structural systems such as investigation of gun voice effect on structures (Jiang and Shu 2005), applicability of similarity theory on designed small scaled models (Ramu *et al.* 2013), earthquake performance evaluation of a multi-story structure with steel reinforced columns using scaled model (Lu *et al.* 2015), numerical estimation of the distribution of large oil drilling tools with scaled model (Shehadeh *et al.* 2015), increasing of wind resistance in the hurricane regions (Datin and Prevatt 2013), investigation on shaking table tests for earthquake performance of the tunnel using scale models (Chen and Shen 2014, Chen *et al.* 2016), experimental dynamic characteristics extraction of the full-scale systems using scaled frame model results (Altunışık *et al.* 2018) etc. Also, some paper can be found about the dimensional analysis and similarity requirement (Carpinteri and Corrado 2010, Balaguer and Claramonte 2011, Ghosh 2011, Balawi *et al.* 2015, Hafeez and Almaskari 2015).

The paper is organized as follows: Section 2 presents fields and scope of the scaling. Section 3 indicates similarity formulas and dimensional analysis. This section purpose here is to show the relationship between the prototype and the model. In these here, formulas obtains by means of easy a model. Section 4 presents finite element analysis results of different scaled arch dams. In this section is compared finite element analysis results with formulas results obtained in section 4. Finally, Section 5 draws the main conclusions of this study.

## 2. Scaling

### 2.1 Scope and usage area

Scaling is a work that can be done in every area, by

shrinking large elements or systems and by enlarge small elements or systems in a certain way to make it easier to work on. The main purpose of the scaling concept used in many areas is basically the same, and the main purpose is to simplify the work by making the hard and time-consuming systems smaller and simpler to test. The study areas of Civil Engineering are multi-story buildings, dams, airports etc. examining and testing such prototypes is a very expensive, time-consuming and difficult-to-control process. For this reason, it is very easy and convenient to do the desired work on the small models created by scaling the prototype. Due to the similarity between the prototype and the model, the results obtained in the small model will be interpreted so that the behavior of the prototype can be predicted.

### 2.2 Scope and usage area

The aim of similarity analysis is to obtain design information of a large and expensive system by correlating the information obtained from experiments on a small and inexpensive model. The similarity conditions of the systems require that the relevant system parameters be the same, and these systems are controlled by the creation of special equations. Thus, equality or relativity of variables written for a system is valid for all systems. Each variable in a model is proportional with the matching variable in the prototype

The solution of the problems obtains with respect to the results of the analytical and experimental studies. First of all, mathematical model apply to obtain the solution of the problem. Experimental measurements are then made to check the analytical results. Experimental studies, which are an important step in comparing results and confirming correctness, require analysis of appropriate experimental data and careful examination. The main purpose of experimental studies is the most knowledge with the least experiment. This purpose is being used in dimensional analysis as an important means of reaching. Dimensional analysis; is a method used to reduce the number and complexity of experimental variables affecting a physical phenomenon. If an event is based on  $n$  dimensional variables, this event can reduce to  $k$  ( $k < n$ ) dimensionless variables with an appropriate dimensional analysis (URL-1).

Any physical state can be expressed together size and unity. While the dimension describes the measurable physical size, the unit is important in terms of describing the intensity of this physical size. When doing dimensional analysis character is much more important than the quantity of physical size. For this reason, only dimensions are taken into consideration in dimensional analysis. The size of each physical size is expressed by the size and symbol of the basic sizes (Table 1). Thus, all dimensions can be collected and processed in the same way.

In its broadest terms, there are two main ways to relate the model to the prototype. Similarity conditions are derived from the relevant field equations if the system has a mathematical model or by dimensional analysis if the mathematical model of the system is not valid. In dimensional analysis, all parameters and variables that affect the behavior of the system have to be known. The

Table 1 Units of some size according to the FLT and MLT systems

	FLT System	MLT System
Gravity	$LT^{-2}$	$LT^{-2}$
Angle	$F^0L^0T^0$	$M^0L^0T^0$
Area	$L^2$	$L^2$
Density	$FL^{-4}T^2$	$ML^{-3}$
Force	$F$	$MLT^{-2}$
Frequency	$T^{-1}$	$T^{-1}$
Length	$L$	$L$
Mass	$FL^{-1}T^2$	$M$
Modulus of Elasticity	$FL^{-2}$	$ML^{-1}T^{-2}$
Moment of force	$FL$	$ML^2T^{-2}$
Moment of inertia	$L^4$	$L^4$
Specify Weight	$FL^{-3}$	$ML^{-2}T^{-2}$
Strain	$F^0L^0T^0$	$M^0L^0T^0$
Stress	$FL^{-2}$	$ML^{-1}T^{-2}$
Time	$T$	$T$
Velocity	$LT^{-1}$	$LT^{-1}$
Volume	$L^3$	$L^3$

obtained equation is the dimensionless product of system parameters and variables. Thus, similarity conditions can be created on the basis of the generated equation.

### 2.3 Buckingham $\Pi$ theorem

There are many methods used to form equations by dimensional analysis. The most widely used of these methods is the Buckingham  $\Pi$  Theorem. If the number of physical quantities (velocity, density, etc.) in a system is  $n$  and the number of basic dimensions (M, L, T) constituting these physical quantities is  $r$ , there is  $k=n-r$  dimensionless number ( $\Pi$  group) that defining the system. In other words, the physical quantities that make up a system (Prabhu *et al.* 2013)

$$f = (A_1, A_2, A_3, \dots, A_i, \dots, A_n) = 0 \quad (1)$$

When represented by the Eq. (1), indicating the relationship between variables  $\Pi$  groups

$$F = (\Pi_1, \Pi_2, \Pi_3, \dots, \Pi_i, \dots, \Pi_{n-r}) = 0 \quad (2)$$

are represented by the Eq. (2). Each  $\Pi$  group is determined to be a function of  $r$  repeating variables that directly affect the physical problem and at least one different variable (Ramu *et al.* 2013).

There are some situations that need to be taken into account choosing the parameters when forming the dimensionless  $\Pi$  groups. Selection unnecessary parameters that are not important for the physical problem can lead to the formation of an extra  $\Pi$  group. On the other hand, is not selecting parameters that are important for the physical problem can lead an important  $\Pi$  group will be overlooked and the interpretation of the results may be lacking.

Table 2 Units of selected parameters according to the  $M, L, T$ 

$a$	$b$	$h$	$m$	$E$	$I$	$k$	$f$
$L$	$L$	$L$	$M$	$ML^{-1}T^{-2}$	$L^4$	$MT^{-2}$	$T^{-1}$

### 3. Similarity formulas by dimensional analysis

Dimensional analysis is carried out by taking into consideration the described points in Buckingham  $\Pi$  Theorem. The purpose here is to show the relationship between the prototype and the model. In order to compare the results of the dimensional analysis, it is first to formulate the frequency change in the columns with the cross-sectional dimensions and height  $a, b, c$ , respectively by Buckingham  $\Pi$  theorem. In the calculation of the frequency value, Eq. (3) and different forms of this equation are used.

$$f_n = \frac{\omega_n}{2\pi}, \quad \omega_n = \sqrt{\frac{k}{m}}, \quad k = \frac{XEI}{h^3} \quad (3)$$

Parameters related to these equations;  $m$  mass,  $k$  rigidity,  $\pi$  dimensionless parameter,  $E$  elasticity modulus,  $I$  inertia moment and  $X$  constant value. The process steps applied according to the Buckingham  $\Pi$  theorem are presented below.

Step 1: Determination of the number of parameters ( $n$ )

The parameters determined according to the frequency formula and their units in terms of  $M, L, T$  are given in Table 2. There are total 8 parameters ( $n=8$ ).

Step 2: Identification of the limiter number ( $r$ )

The rules expressed in the selection of  $r$ , which is the number of repeating parameters and the frequency formula given in Eq. (3) are taken into account and are chosen as  $r=(E, h, m)$ . These basic parameters do not consist combination of different parameters.

Step 3: Determination of the non-repeating parameter number ( $k$ ) and  $\Pi$ -group number

There are 5 number of  $\Pi$ -groups for  $k=n-r$ . When represented by the Eq. (2)

$$f = (\pi_1, \pi_2, \pi_3, \pi_4, \pi_5) = 0 \quad (4)$$

Eq. (4) is obtained. In this way, each non-repeating parameter  $\pi_1=f, \pi_2=a, \pi_3=b, \pi_4=I$  and  $\pi_5=k$ , is determined.

Each non-repeating parameter can be obtained as follows (Eq. (5))

$$\left. \begin{aligned} \pi_1 &= f. (E^a . h^b . m^c) \\ \pi_2 &= a. (E^a . h^b . m^c) \\ \pi_3 &= b. (E^a . h^b . m^c) \\ \pi_4 &= I. (E^a . h^b . m^c) \\ \pi_5 &= k. (E^a . h^b . m^c) \end{aligned} \right\} \quad (5)$$

In order for groups to be dimensionless, the basic condition of  $M^0L^0T^0$  must also be provided for  $\pi_1$

$$\left. \begin{aligned} \pi_1 &= f.(E^a.h^b.m^c) \\ M^0L^0T^0 &= L.(ML^{-1}T^{-2})^a.L^b.M^c \end{aligned} \right\} \quad (6)$$

expressions are obtained (Eq. (6)). The coefficients of  $a$ ,  $b$ ,  $c$  are obtained when the equation is solved considering the fact that the upper force of the same basic dimension is the same on both sides of the equation. When each parameter is calculated in all  $\Pi$ -groups, the final part is obtained as follows.

$$\left. \begin{aligned} \pi_{1(model)} &= \pi_{1(prototype)} \\ \pi_{2(model)} &= \pi_{2(prototype)} \\ \pi_{3(model)} &= \pi_{3(prototype)} \\ \pi_{4(model)} &= \pi_{4(prototype)} \\ \pi_{5(model)} &= \pi_{5(prototype)} \end{aligned} \right\} \quad (7)$$

With Eq. (7), the relation between prototype and model is established and solutions of  $\Pi$ -groups are made respectively.

➤ for  $\pi_1=f.(E,h,m)$ ;

$$\left. \begin{aligned} \pi_{1(model)} &= \pi_{1(prototype)} \\ \pi_{2(model)} &= \pi_{2(prototype)} \\ \pi_{3(model)} &= \pi_{3(prototype)} \\ \pi_{4(model)} &= \pi_{4(prototype)} \\ \pi_{5(model)} &= \pi_{5(prototype)} \end{aligned} \right\} \quad (8)$$

$a = -\frac{1}{2}, c = \frac{1}{2}$  and  $b = -\frac{1}{2}$  are obtained in Eq. (8).

When the relevant expressions are written to

$$\left. \begin{aligned} \pi_1 &= f.\left(E^{-\frac{1}{2}}.h^{-\frac{1}{2}}.m^{\frac{1}{2}}\right) \\ \pi_1 &= \frac{f\sqrt{m}}{\sqrt{E}\sqrt{h}} \\ \pi_{1(model)} &= \pi_{1(prototype)} \end{aligned} \right\} \quad (9)$$

expressions are obtained (Eq. (9)). When considering that  $m$  and  $p$  represent the model and the prototype, respectively, it's expression of the equation

$$\left. \begin{aligned} \frac{f_m\sqrt{m_m}}{\sqrt{E_m}\sqrt{h_m}} &= \frac{f_p\sqrt{m_p}}{\sqrt{E_p}\sqrt{h_p}} \\ \frac{f_m}{f_p} &= \frac{\sqrt{m_p}}{\sqrt{m_m}} \frac{\sqrt{E_m}}{\sqrt{E_p}} \frac{\sqrt{h_m}}{\sqrt{h_p}} \end{aligned} \right\} \quad (10)$$

its occurs. Eq. (10) is shown as the scale factor of the frequency. Also

$$f_m = \frac{\sqrt{m_p}}{\sqrt{m_m}} \frac{\sqrt{E_m}}{\sqrt{E_p}} \frac{\sqrt{h_m}}{\sqrt{h_p}} f_p \quad (11)$$

Table 3 Scale factors

$\frac{f_m}{f_p}$	$\frac{\sqrt{m_p}}{\sqrt{m_m}} \frac{\sqrt{E_m}}{\sqrt{E_p}} \frac{\sqrt{h_m}}{\sqrt{h_p}}$
$\frac{a_m}{a_p}$	$\frac{1}{S}$
$\frac{b_m}{b_p}$	$\frac{1}{S}$
$\frac{I_m}{I_p}$	$\frac{1}{S^4}$
$\frac{k_m}{k_p}$	$\frac{1}{ES}$

The frequency of the model with the equation is obtained depend on the prototype frequency and the parameters (Eq. (11)). The same procedures for  $\pi_2, \pi_3, \pi_4$  and  $\pi_5$  are repeated and each of the scale factors presented in Table 3. Where;  $S$  is the length scale factor.

According to the different scaling, the changes in general formula is obtained by Buckingham  $\Pi$  theorem. With the aid of the mathematical formula of frequency, dimensional analysis is carried out with different combinations according to geometric, mass and material scales and the results obtained are examined comparatively.

√ The solution of the column prototype with the help of the mathematical formula is summarized as follows;

Column dimensions  $a \times b \times 1$  m

Other data in the system  $\gamma, E_p, g$  ;

$$\text{System rigidity } k = \frac{12 E_p}{L^3}$$

$$\left. \begin{aligned} I &= \frac{ab^3}{12} \\ k &= \frac{12E_p}{L^3} \frac{ab^3}{12} = \frac{12E_p ab^3}{12L^3} = \frac{E_p ab^3}{L^3} \\ m &= \frac{abL\gamma}{g} \\ \omega_n &= \sqrt{\frac{k}{m}} = \sqrt{\frac{E_p ab^3}{L^3} \frac{g}{abL\gamma}} = \sqrt{\frac{E_p b^2 g}{L^4 \gamma}} \\ f_{n(prototype)} &= \frac{\omega_n}{2\pi} = \frac{1}{2\pi} \sqrt{\frac{E_p b^2 g}{L^4 \gamma}} \end{aligned} \right\} \quad (12)$$

The corresponding solution can be made as follows and Eq. (12) is obtained. For the different scaled model situations of the column, the following steps are performed with the help of mathematical model.

√ By considering the mass change, in the case of  $1/S$  geometry and material scaling;

Column dimensions  $\frac{a}{S} \times \frac{b}{S} \times \frac{1}{S}$  m

Other data in the system  $\gamma, E_m, g$

as considering data, the corresponding solution can be made as follows and

Table 4 Frequency formulas for different scaling obtained by similarity requirement

Scale	Formulas
Geometry	$f_{n(m)} = \frac{1}{\sqrt{S}} f_{n(p)}$
Geometry and Mass	$f_{n(m)} = S f_{n(p)}$
Material	$f_{n(m)} = \sqrt{\frac{E_m}{E_p}} f_{n(p)}$
Geometry and material	$f_{n(m)} = \frac{1}{\sqrt{S}} \sqrt{\frac{E_m}{E_p}} f_{n(p)}$
Geometry, Material and Mass	$f_{n(m)} = S \sqrt{\frac{E_m}{E_p}} f_{n(p)}$

$$\begin{aligned}
 I &= \frac{a \left( \frac{b}{S} \right)^3}{12} = \frac{ab^3}{S^4 12} \\
 k &= \frac{12E_m \frac{ab^3}{S^4 12}}{\left( \frac{L}{S} \right)^3} = \frac{12E_m ab^3 S^3}{12S^4 L^3} = \frac{E_m ab^3}{L^3} \frac{1}{S} \\
 m &= \frac{abL}{SSS} \gamma = \frac{abL\gamma}{S^3 g} = \frac{abL\gamma}{g} \frac{1}{S^3} \\
 \omega_n &= \sqrt{\frac{k}{m}} = \sqrt{\frac{E_m ab^3 \frac{1}{S} \frac{g}{abL\gamma} \frac{S^3}{1}}{L^4 \gamma}} = \sqrt{\frac{E_m b^2 g}{L^4 \gamma}} S \\
 f_{n(\text{Model})} &= \frac{\omega_n}{2\pi} = \sqrt{\frac{E_m b^2 g}{L^4 \gamma}} \frac{1}{2\pi} S
 \end{aligned} \quad (13)$$

Eq. (13) is obtained. By establishing a relationship between the prototype and the scaled model of the column

$$\frac{f_{n(\text{Model})}}{f_{n(\text{prototype})}} = \frac{\sqrt{E_m} S}{\sqrt{E_p}} \Rightarrow f_{n(m)} = S \sqrt{\frac{E_m}{E_p}} f_{n(p)} \quad (14)$$

Equality is reached (Eq. (14)). The frequency formulas obtained according to different scale using the equations and expressions tried to be explained in detail above are summarized in Table 4.

When the obtained equations are evaluated, it is seen that the frequency relations obtained from Buckingham II theorem and field equations are the same. In the most general way, when is written prototype and model data in the Eq. (10), the frequency value of the scaled model is obtained. It is also possible to convert the data into different formats. When conversion is done for mass (Eq. (15))

$$\left. \begin{aligned}
 m &= V \cdot \gamma \\
 m_p &= V_p \cdot \gamma_p \\
 m_m &= V_m \cdot \gamma_m
 \end{aligned} \right\} \quad (15)$$

If the expressions are written in Eq. (10)

$$f_m = \frac{\sqrt{V_p \gamma_p}}{\sqrt{V_m \gamma_m}} \frac{\sqrt{E_m}}{\sqrt{E_p}} \frac{\sqrt{h_m}}{\sqrt{h_p}} f_p \quad (16)$$

Eq. (16) is obtained. When converting for volume

$$\left. \begin{aligned}
 V &= a \cdot b \cdot h \quad (br^3) \\
 V_p &= a_p \cdot b_p \cdot h_p \\
 V_m &= a_m \cdot b_m \cdot h_m
 \end{aligned} \right\} \quad (17)$$

If the expressions in Eq. (17) are written in Eq. (10)

$$\left. \begin{aligned}
 f_m &= \frac{\sqrt{a_p \cdot b_p \cdot h_p \cdot \gamma_p}}{\sqrt{a_m \cdot b_m \cdot h_m \cdot \gamma_m}} \frac{\sqrt{E_m}}{\sqrt{E_p}} \frac{\sqrt{h_m}}{\sqrt{h_p}} f_p \\
 f_m &= \frac{\sqrt{a_p \cdot b_p \cdot h_p}}{\sqrt{a_m \cdot b_m \cdot h_m}} \frac{\sqrt{\gamma_p}}{\sqrt{\gamma_m}} \frac{\sqrt{E_m}}{\sqrt{E_p}} \frac{\sqrt{h_m}}{\sqrt{h_p}} f_p
 \end{aligned} \right\} \quad (18)$$

is obtained. Volume scale factor  $S^3$  is written in formula obtained with Eq. (18)

$$\left. \begin{aligned}
 f_m &= \frac{\sqrt{S^3}}{1} \frac{\sqrt{\gamma_p}}{\sqrt{\gamma_m}} \frac{\sqrt{E_m}}{\sqrt{E_p}} \frac{1}{\sqrt{S}} f_p \\
 f_m &= S \frac{\sqrt{\gamma_p}}{\sqrt{\gamma_m}} \frac{\sqrt{E_m}}{\sqrt{E_p}} f_p
 \end{aligned} \right\} \quad (19)$$

Eq. (19) is obtained. Conclusions can be obtained with different density values  $\gamma$  in formula obtained.

The weight of the build varies with the scale. In the scale study, the constant mass status is formed by adding to the structure as extra load the mass loss formed by volume reduction. Different equations can be obtained by keeping the desired parameter scaled.

The equations obtained by using the column model are generalized by simplifying of the column model specific coefficients and obtaining the basic parameters, and these equations can be used in every system.

In order to obtain the displacement relations, similarity conditions are formed according to different scale using mathematical models. Using the general displacement equation, the relationship between the prototype and the scaled model for the column

$$\begin{aligned}
 F &= K \cdot U \\
 F &= V \cdot \gamma \\
 k &= \frac{12EI}{L^3}
 \end{aligned} \quad (20)$$

using the expressions given in Eq. (20), for prototype

$$V_p \cdot \gamma_p = \frac{12E_p I_p}{L_p^3} U_p \quad (21)$$

for model

$$V_m \cdot \gamma_m = \frac{12E_m I_m}{L_m^3} U_m \quad (22)$$

Eqs. (21-22) are obtained. When  $\frac{U_p}{U_m}$  similarity

condition is applied

$$\frac{U_p}{U_m} = \frac{E_m I_m L_p^3 V_p \gamma_p}{E_p I_p L_m^3 V_m \gamma_m} \quad (23)$$

Table 5 Displacement formulas considering different types of scaling

Scale	Formulas
Geometry	$\delta_m = S \delta_p$
Geometry and Mass	$\delta_m = \frac{1}{S^2} \delta_p$
Material	$\delta_m = \frac{E_p}{E_m} \delta_p$
Geometry and material	$\delta_m = \frac{E_p}{E_m} S \delta_p$
Geometry, Material and Mass	$\delta_m = \frac{E_p}{E_m} \frac{1}{S^2} \delta_p$

Eq. (23) is obtained. When the scale factor for the moment of inertia is taken as  $S^4$

$$\left. \begin{aligned} \frac{U_p}{U_m} &= \frac{E_m}{E_p} \frac{1}{S^4} S^3 \frac{V_p \gamma_p}{V_m \gamma_m} \\ \frac{U_p}{U_m} &= \frac{E_m}{E_p} \frac{1}{S} \frac{V_p \gamma_p}{V_m \gamma_m} \end{aligned} \right\} \quad (24)$$

A general similarity formula (Eq. (24)) is obtained for the displacement. In the equation, when the scale factor for volume  $S^3$  is written

$$\left. \begin{aligned} \frac{U_p}{U_m} &= \frac{E_m}{E_p} \frac{1}{S} S^3 \frac{\gamma_p}{\gamma_m} \\ U_m &= \frac{E_p}{E_m} \frac{1}{S^2} \frac{\gamma_m}{\gamma_p} U_p \end{aligned} \right\} \quad (25)$$

Eq. (25) is obtained. The displacement value of the scaled model is obtained by writing the prototype displacement values in Eq. (25). The corresponding formulas are summarized in Table 5 considering different types of scaling.

In order to obtain the stress relations, similarity conditions are performed according to different scale using mathematical models. Using the general stress formula presented in Eq. (26), the relationship between the prototype and scaled model

$$\sigma = \frac{F}{A} = \frac{V \gamma}{A} \quad (26)$$

for prototype and model

$$\sigma_p = \frac{V_p \gamma_p}{A_p} \quad (27)$$

$$\sigma_m = \frac{V_m \gamma_m}{A_m} \quad (28)$$

Eqs. (27)-(28) are obtained, respectively. Where;  $\sigma$ ,  $V$ ,  $\gamma$  and  $A$  are stress, volume, density and area, respectively. With the ratio of these two equations

$$\left. \begin{aligned} \frac{\sigma_p}{\sigma_m} &= \frac{V_p \gamma_p}{A_p} \frac{A_m}{V_m \gamma_m} \\ \frac{\sigma_p}{\sigma_m} &= \frac{V_p}{V_m} \frac{\gamma_p}{\gamma_m} \frac{A_m}{A_p} \end{aligned} \right\} \quad (29)$$

A general similarity formula is obtained for the stress (Eq. (29)). In the equation, when the scale factors for volume  $S^3$  and area  $S^2$  are written

$$\left. \begin{aligned} \frac{\sigma_p}{\sigma_m} &= S^3 \frac{\gamma_p}{\gamma_m} \frac{1}{S^2} \\ \sigma_m &= \frac{1}{S} \frac{\gamma_m}{\gamma_p} \sigma_p \end{aligned} \right\} \quad (30)$$

Eq. (30) is obtained. In order to obtain the strain relations, similarity conditions are performed according to different scale using mathematical models. Using the general strain formula presented in Eq. (31), the relationship between the prototype and the scaled model

$$\left. \begin{aligned} \sigma &= E \varepsilon \\ \varepsilon &= \frac{\sigma}{E} \end{aligned} \right\} \quad (31)$$

for prototype and model

$$\varepsilon_p = \frac{\sigma_p}{E_p} \quad (32)$$

$$\varepsilon_m = \frac{\sigma_m}{E_m} \quad (33)$$

Eqs. (32)-(33) are obtained. Where;  $\varepsilon$ ,  $\sigma$ ,  $V$ ,  $\gamma$  and  $A$  are strain, stress, volume, density and area, respectively. With the ratio of these two equations

$$\left. \begin{aligned} \frac{\varepsilon_p}{\varepsilon_m} &= \frac{\sigma_p}{\sigma_m} \frac{E_m}{E_p} \\ \frac{\varepsilon_p}{\varepsilon_m} &= \frac{V_p}{V_m} \frac{\gamma_p}{\gamma_m} \frac{A_m}{A_p} \frac{E_m}{E_p} \end{aligned} \right\} \quad (34)$$

A general similarity formula is obtained for the strain (Eq. (34)). In the equation, when the scale factors for volume  $S^3$  and area  $S^2$  are written and Eq. (35) is obtained.

$$\left. \begin{aligned} \frac{\varepsilon_p}{\varepsilon_m} &= S \frac{\gamma_m}{\gamma_p} \frac{E_m}{E_p} \\ \varepsilon_m &= \frac{1}{S} \frac{\gamma_p}{\gamma_m} \frac{E_p}{E_m} \varepsilon_p \end{aligned} \right\} \quad (35)$$

#### 4. Type-1 arch dam

There are five types of arch dams with different geometries proposed in the symposium "Arch Dams (1968)" held in England in 1968. Among these dam types,

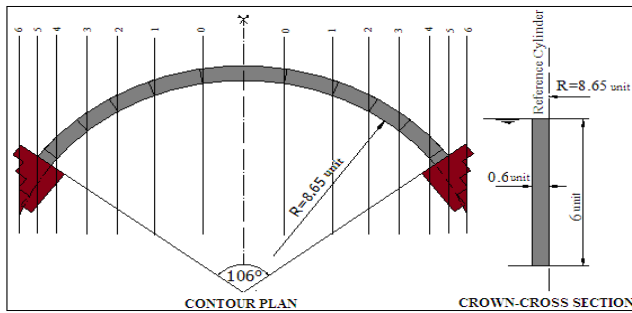


Fig. 1 Geometrical properties of Type-1 arch dam

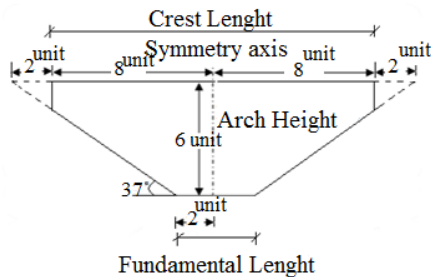


Fig. 2 The cross-section of the valley where the Type-1 arch dam is located

Type-1 arch dam is selected in order to construct the laboratory model. The Type-1 arch dam has geometry that a constant radius, angle and a single curvature.

The geometrical characteristics of the Type-1 arch dam are shown in Fig. 1. The Type-1 arch dam, with a fixed center of  $106^\circ$  and a fixed radius of 8.65 units, is a symmetrical dam whose downstream face is considered as a reference. Type-1 arch dam is of 6 units in height, crest and base width of 0.6 units. It is assumed that the cross-section is placed on a valley with a trapezoidal cross-section as shown in Fig. 2 (Arch Dams 1968). The valley where the Type-1 arch dam is located has of 16 units at the crest level and of 4 units at the base level.

#### 4.1 Constitution of laboratory model

In the Type-1 arch dam whose dimensions are given in units, 1 unit=10 cm is selected and the laboratory model is built. According to the obtained data, the dam height (H) is 60cm, the crest and the base width are 6 cm and the crest length of the dam is calculated as 171.13 cm in the upstream face and 160.03 cm in the downstream face. The dam model has been developed including dam-reservoir-foundation interaction to realistically determine the dynamic response of the Type-1 arch dam (Sevim 2010). Three-dimensional solid model is given with dimensions in Fig. 3. Fig. 4 shows the some photographs during construction phase.

#### 4.2 Numerical and experimental measurements

Non-destructive experimental measurements such as ambient vibration and forced vibration tests are conducted on the dam body to extract the natural frequencies. Table 6 summarizes the first nine numerically and experimentally identified natural frequencies.

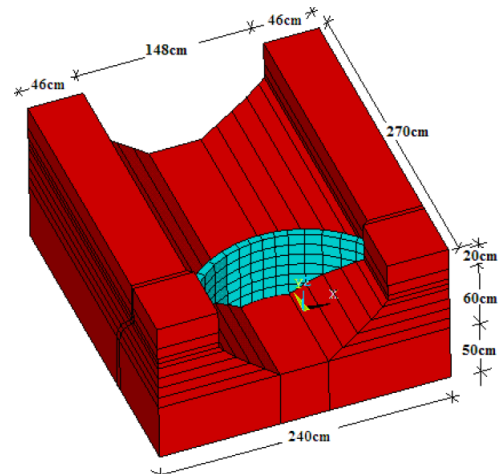


Fig. 3 Three dimensional solid model of Type-1 arch dam (Sevim 2010)



Fig. 4 Some photographs during construction (Sevim 2010)

Table 6 Numerical and experimental first nine natural frequencies

Mode Number	Frequency Values (Hz)		
	Finite Element Analysis	Ambient Vibration Test	Forced Vibration test
1	348.87	339.2	340
2	364.81	372.6	372
3	510.22	552.3	552
4	658.45	619.8	616
5	680.42	----	----
6	701.66	----	----
7	740.70	741.1	740
8	793.32	----	----
9	836.73	839.0	828

#### 4.3 Finite element analysis

In order to verify the results given in Table 6 and obtain the displacements with principal stresses and strain, finite element model of the Type-1 arch dam is constituted in ANSYS software (2016). It is aimed to use these results as an initial and references parameters for scaling.

The analyses are carried out both fixed support and dam-foundation interaction conditions. Empty reservoir condition is taken into consideration. For the next studies, it is aim to investigate the reservoir and dynamic load effects on structural response. Modal analyses are done and first

Table 7 Dynamic characteristics of Type-1 arch dam for dam-foundation interaction

Mode Number	Finite Element Analysis Results		
	Frequency (Hz)	Period (s)	Mode Shape
1	344.58706	0.002020	Anti-Symmetrical Mode
2	361.20676	0.002768	Symmetrical Mode
3	505.56430	0.001978	Symmetrical Mode
4	652.08387	0.001534	Anti-Symmetrical Mode
5	674.36188	0.001483	Vertical Mode
6	860.11709	0.001163	Vertical Mode
7	890.79624	0.001125	Symmetrical Mode
8	917.23440	0.001090	Vertical Mode
9	954.16860	0.001048	Symmetrical mode
10	958.79734	0.001043	Symmetrical mode

Table 8 Dynamic characteristics of Type-1 arch dam for fixed support condition

Mode Number	Finite Element Analysis Results		
	Frequency (Hz)	Period (s)	Mode Shape
1	362.74	0.0028161	Anti-Symmetrical Mode
2	376.40	0.0027139	Symmetrical Mode
3	525.12	0.0019453	Symmetrical Mode
4	679.00	0.0015044	Anti-Symmetrical Mode
5	698.13	0.0014632	Vertical Mode
6	904.96	0.0011288	Vertical Mode
7	923.45	0.0011062	Symmetrical Mode
8	1196.0	0.0008541	Vertical Mode
9	1231.8	0.0008293	Symmetrical mode
10	1235.2	0.0008270	Symmetrical mode

ten natural frequencies, period values and mode shapes are obtained. Tables 7 and 8 present the related results. In the finite element analysis, the material properties are selected as  $E=150000$  MPa for dam body and foundation according to the updated finite element results by experimental measurement.

Static analyses of the Type-1 arch dam are carried out under its own weight considering empty reservoir water both fixed support and dam-foundation interaction conditions. Displacements, principal stresses and principal strains are calculated at the all nodal points of upstream and downstream faces (Fig. 5) of dam body. A total of 346 nodal points are located on the upstream and downstream faces of dam body. 10 critical nodal points are selected to display the changes of displacements and internal forces. Tables 9 and 10 present the displacements, Table 11 presents the maximum and minimum principal stresses, and Table 12 presents the maximum and minimum principal strains values obtained from the static analysis of Type-1 arch dam for both structural condition in order to compare these results more accurately.

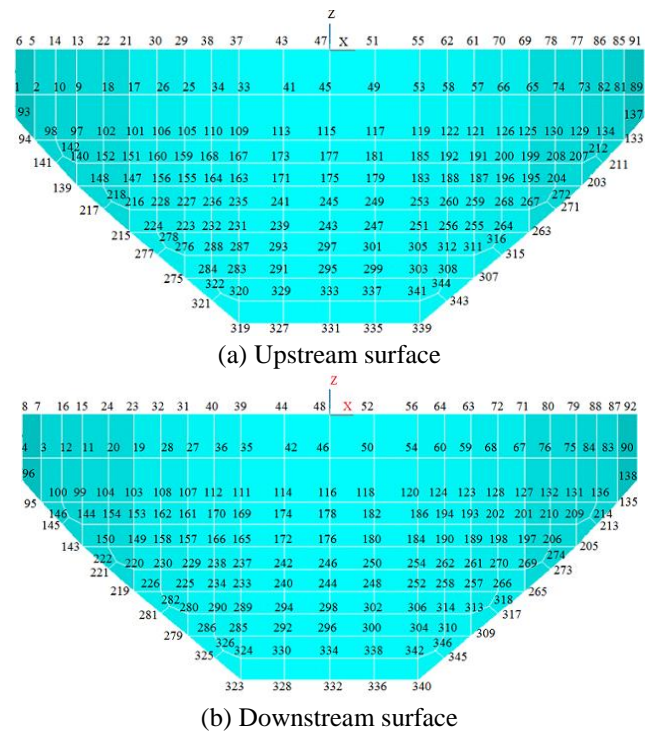


Fig. 5 Nodal points on upstream and downstream faces of Type-1 arch dam

Table 9 Displacements obtained from static analysis for dam-foundation interaction

Nodal Points	Displacements (cm)		
	Crest Direction	Upstream-Downstream Direction	Vertical Direction
48	7.8151E-20	1.7834E-05	-5.3070E-05
103	3.1855E-07	5.5562E-06	-4.4862E-05
115	2.3717E-20	1.3267E-05	-5.1530E-05
125	7.0024E-07	5.3223E-06	-4.5459E-05
169	-4.6662E-07	9.6484E-06	-4.7358E-05
185	1.5728E-06	9.8743E-06	-4.8836E-05
238	-7.9775E-07	5.5382E-06	-4.2099E-05
246	9.8158E-20	8.3769E-06	-4.3518E-05
260	1.9853E-06	5.8581E-06	-4.3770E-05
332	2.2340E-20	1.8290E-07	-2.6190E-05

### 5. Determination of real arch dam model results

Finite element analyses, experimental measurements, similarity requirements and scaling laws given in the previous sections show the correctness of prototype Type-1 arch dam. Its mean that finite element models and its analyses can be safely used to predict the structural response of arch dams with different dimensions and material properties. To investigate the real arch dam response using scaling laws and similarity requirements with related formulas, four different arch dam (Model-1, Model-2, Model-3 and Model-4) are selected as an example. Fig. 6 shows the some photos from these arch dams including construction years.

The experimental natural frequencies extracted using

Table 10 Displacements obtained from static analysis for fixed support condition

Nodal Points	Displacements (cm)		
	Crest Direction	Upstream-Downstream Direction	Vertical Direction
48	-1.4647E-19	3.0146E-05	-2.2164E-05
103	3.7272E-06	1.5754E-06	-9.3188E-06
115	1.7788E-20	2.0645E-05	-2.2550E-05
125	-2.5929E-06	1.2345E-06	-8.8506E-06
169	1.5256E-06	1.2330E-05	-1.5822E-05
185	1.4175E-06	1.2109E-05	-1.8003E-05
238	1.5023E-06	5.6791E-06	-1.0008E-05
246	-2.6012E-20	1.2182E-05	-1.3890E-05
260	8.4133E-07	5.5834E-06	-1.1964E-05
332	0	0	0

Table 11 Principal stresses obtained from static analysis for both structural conditions

Nodal Points	Dam-Foundation Interaction		Fixed Support Condition	
	Max Principal Stress	Min. Principal Stress	Max Principal Stress	Min. Principal Stress
48	-0.00014200	-0.00118540	-0.000155300	-0.0032515
103	0.00030622	-0.00416980	0.00209600	-0.0042684
115	0.00042557	-0.00403250	0.00110900	-0.0034780
125	0.00000265	-0.00389940	0.00006272	-0.0046365
169	0.00001503	-0.00585250	0.00002708	-0.0054861
185	0.00012880	-0.00527620	0.00048807	-0.0049661
238	0.00002984	-0.00866150	0.00002854	-0.0071746
246	-0.00001120	-0.00844570	-0.00001620	-0.0075281
260	0.00002497	-0.00747870	0.00002407	-0.0073603
332	-0.00135100	-0.00852830	-0.00223850	-0.0085459

Table 12 Principal strains obtained from static analysis for both structural conditions

Nodal Points	Dam-Foundation Interaction		Fixed Support Condition	
	Max Principal Stress	Min. Principal Stress	Max Principal Stress	Min. Principal Stress
48	1.5484E-08	-6.7991E-08	4.9696E-08	-1.9800E-07
103	7.5816E-08	-2.8226E-07	1.9575E-07	-3.2961E-07
115	8.2162E-08	-2.7448E-07	1.2043E-07	-2.6378E-07
125	5.3448E-08	-2.5871E-07	6.6524E-08	-3.0941E-07
169	8.5846E-08	-3.8356E-07	8.7642E-08	-3.5341E-07
185	7.8758E-08	-3.5364E-07	9.8610E-08	-3.3772E-07
238	1.1440E-07	-5.1575E-07	1.0287E-07	-4.7338E-07
246	1.2372E-07	-5.5104E-07	1.2493E-07	-4.7602E-07
260	1.0653E-07	-4.9376E-07	1.0459E-07	-4.8616E-07
332	6.1314E-08	-5.1287E-07	2.6227E-07	-8.9783E-07

ambient vibration tests considering dam-reservoir-foundation interaction in the previous studies are presented in Table 13.

Table 14 present the detail information such as scaling factors, arch heights, arch interior radius and thickness with modulus of elasticity considered in the analyses to reflect the real arch dam models (Model-1, Model-2, Model-3 and Model-4).



Fig. 6 Some photos from the selected arch dam including construction years

Table 13 Experimental frequency values of arch dams selected for study

Frequencies (Hz)	Berke Arch Dam (Sevim <i>et al.</i> 2009)	Deriner Arch Dam (Başbolat <i>et al.</i> 2013)
1	2.75	1.658
2	3.41	2.331
3	4.81	3.045
4	5.34	3.757
5	6.25	4.467
6	7.94	----
7	8.63	----
8	9.64	----

Table 14 Geometrical properties of Type-1 arch dam and scaled arch dam models

Type-1 Arch Dam	Scale	Arch Height (m)	Arch Interior Radius (m)	Crest and Fundamental Thickness (m)	Modulus of Elasticity (MPa)
Prototype	1	0.60	0.8650	0.06	15000
Model-1	335	201	289.78	20.1	34000
Model-2	400	240	346.00	24.0	34000
Model-3	416.67	250	360.42	25.0	34000
Model-4	450	270	389.25	27.0	34000

Considering the frequency values of prototype Type-1 arch dam given in Table 7 including dam-foundation interaction, the first natural frequencies of Model-1 and Model-2 are calculated using Eq. (19) as

$$f_{m_1} = \frac{1}{S} \frac{\sqrt{\gamma_p} \sqrt{E_{m_1}}}{\sqrt{\gamma_{m_1}} \sqrt{E_p}} f_p \quad \left. \vphantom{f_{m_1}} \right\} (36)$$

$$f_{m_1} = \frac{1}{335} \frac{\sqrt{2300} \sqrt{34000}}{\sqrt{2300} \sqrt{15000}} 344.58706 = 1.548611 \text{ Hz}$$

Table 15 The first ten natural frequencies of scaled arch dam models using FE analyses and formula for dam-foundation interaction

Mode Numbers	Frequency (Hz)							
	Model-1		Model-2		Model-3		Model-4	
	ANSYS	Formula	ANSYS	Formula	ANSYS	Formula	ANSYS	Formula
1	1.5486	1.5486311	1.297	1.2969786	1.2451	1.2450895	1.1529	1.1528698
2	1.6233	1.6233228	1.3595	1.3595329	1.3051	1.3051411	1.2085	1.2084736
3	2.2721	2.2720894	1.9029	1.9028749	1.8267	1.8267453	1.6914	1.6914444
4	2.9306	2.9305726	2.4544	2.4543545	2.3562	2.3561615	2.1816	2.1816485
5	3.0307	3.0306936	2.5382	2.5382059	2.4367	2.4366582	2.2562	2.256183
6	3.8655	3.8655082	3.2374	3.2373631	3.1078	3.1078437	2.8777	2.8776561
7	4.0034	4.0033854	3.3528	3.3528352	3.2187	3.2186961	2.9803	2.980298
8	4.1222	4.1222028	3.4523	3.4523449	3.3142	3.3142246	3.0688	3.068751
9	4.2882	4.2881912	3.5914	3.5913601	3.4477	3.4476782	3.1923	3.1923201
10	4.309	4.3089935	3.6088	3.6087821	3.4644	3.4644031	3.2078	3.2078063

Table 16 The first ten natural frequencies of scaled arch dam models using FE analyses and formula for fixed support condition

Mode Numbers	Frequency (Hz)							
	Model-1		Model-2		Model-3		Model-4	
	ANSYS	Formula	ANSYS	Formula	ANSYS	Formula	ANSYS	Formula
1	1.6302	1.63021345	1.3653	1.365304	1.3107	1.3106811	1.2136	1.2136033
2	1.6916	1.69160374	1.4167	1.416718	1.36	1.3600385	1.2593	1.259305
3	2.36	2.35997597	1.9765	1.97648	1.8974	1.8974055	1.7569	1.756871
4	3.0515	3.0515381	2.5557	2.555663	2.4534	2.453417	2.2717	2.2717006
5	3.1375	3.13751147	2.6277	2.627666	2.5225	2.522539	2.3357	2.335703
6	4.0671	4.06703964	3.4062	3.406146	3.2699	3.2698737	3.0277	3.0276851
7	4.1501	4.15013675	3.4757	3.47574	3.3367	3.3366833	3.0895	3.0895462
8	5.3751	5.37502145	4.5017	4.50158	4.3216	4.3214827	4.0015	4.0014049
9	5.5361	5.53591256	4.6365	4.636327	4.451	4.4508381	4.1213	4.1211793
10	5.5513	5.55119272	4.6492	4.649124	4.4632	4.4631232	4.1326	4.1325546

$$\left. \begin{aligned} f_{m_2} &= \frac{1}{S} \frac{\sqrt{\gamma_p}}{\sqrt{\gamma_{m_2}}} \frac{\sqrt{E_{m_2}}}{\sqrt{E_p}} f_p \\ f_{m_1} &= \frac{1}{400} \frac{\sqrt{2300}}{\sqrt{2300}} \frac{\sqrt{34000}}{\sqrt{15000}} 344.58706 = 1.2969786 \text{ Hz} \end{aligned} \right\} (37)$$

Tables 15 and 16 present the first ten natural frequencies of scaled arch dam models (Model-1, Model-2, Model-3 and Model-4) using finite element analysis and related formula both dam-foundation interaction and fixed support condition. It can be seen from these tables that there is a good agreement between finite element results and related formula.

For the displacement results, scale factor between prototype structure and scaled models is taken into consideration as  $\frac{1_m}{1_p} = \frac{1}{S}$ . In this paper, the terms of

prototype and model are used to emphasize the laboratory arch dam model and real constructed or under construction arch dam structures, respectively. So, Eq. (25) is rearranged as below to obtain the Eq. (38) using corresponding scale factor  $\frac{1_m}{1_p} = S$ .

Considering the displacement values of prototype Type-1 arch dam for upstream-downstream direction given in Table 9 including dam-foundation interaction, the displacement value at 48th nodal point (middle of crest) of Model-1 and Model-2 are calculated using Eq. (38) as

$$U_m = \frac{E_p}{E_m} \frac{\gamma_m}{\gamma_p} S^2 U_p \quad (38)$$

For example, the displacement value at 48th nodal point for Model-1 is obtained as

$$\left. \begin{aligned} U_{m_1} &= \frac{E_p}{E_{m_1}} \frac{\gamma_{m_1}}{\gamma_p} S^2 U_p \\ U_{m_1} &= \frac{15000}{34000} \times \frac{2300}{2300} \times 335^2 \times 1.7834 E - 5 = 0.8830 \text{ cm} \end{aligned} \right\} (39)$$

For example, the displacement value at 48th nodal point for Model-2 is obtained as

$$\left. \begin{aligned} U_{m_2} &= \frac{E_p}{E_{m_2}} \frac{\gamma_{m_2}}{\gamma_p} S^2 U_p \\ U_{m_2} &= \frac{15000}{34000} \times \frac{2300}{2300} \times 400^2 \times 1.7834 E - 5 = 1.258871 \text{ cm} \end{aligned} \right\} (40)$$

All displacements can be obtained using same

Table 17 The displacement values of scaled arch dam models using FE analyses and formula for dam-foundation interaction

Nodal Points	Displacements (cm) [Upstream-Downstream Direction]							
	Model-1		Model-2		Model-3		Model-4	
	ANSYS	Formula	ANSYS	Formula	ANSYS	Formula	ANSYS	Formula
48	0.88300	0.88298	1.25890	1.258871	1.366	1.3659839	1.5933	1.5932581
103	0.27509	0.275093	0.39220	0.392202	0.42558	0.4255736	0.49638	0.4963811
115	0.65684	0.656863	0.93647	0.936494	1.0161	1.0161774	1.1852	1.1852504
125	0.26351	2.635126	0.37569	0.375692	0.40766	0.4076582	0.47548	0.4754849
169	0.4777	0.477702	0.68106	0.681064	0.73901	0.739013	0.86197	0.861971
185	0.48889	0.488887	0.69701	0.697009	0.75631	0.7563157	0.88215	0.8821525
238	0.27420	0.274202	0.39093	0.390932	0.42419	0.4241949	0.49477	0.494773
246	0.41475	0.414749	0.59131	0.591311	0.64162	0.6416233	0.74838	0.7483775
260	0.29004	0.290041	0.41351	0.413513	0.4487	0.4486974	0.52335	0.5233523
332	0.00906	0.009056	0.01291	0.012911	0.014009	0.0140091	0.01634	0.01634

Table 18 The displacement values of scaled arch dam models using FE analyses and formula for fixed support condition

Nodal Points	Displacements (cm) [Upstream-Downstream Direction]							
	Model-1		Model-2		Model-3		Model-4	
	ANSYS	Formula	ANSYS	Formula	ANSYS	Formula	ANSYS	Formula
48	1.492600	1.492559	2.128000	2.127953	2.309	2.3090137	2.6932	2.6931904
103	0.077997	0.078	0.111200	0.111205	0.12066	0.1206668	0.14074	0.1407435
115	1.022100	1.022155	1.457300	1.457294	1.5813	1.5812906	1.8444	1.8443879
125	0.061123	0.061121	0.087143	0.087141	0.094558	0.0945557	0.11029	0.1102881
169	0.610480	0.610471	0.870370	0.870353	0.94443	0.9444085	1.1016	1.1015404
185	0.599550	0.599529	0.854780	0.854753	0.92751	0.9274811	1.0818	1.0817967
238	0.281180	0.281178	0.400870	0.400878	0.43498	0.434987	0.50736	0.5073608
246	0.603130	0.603143	0.859890	0.859906	0.93305	0.9330725	1.0883	1.0883184
260	0.276440	0.27644	0.394120	0.394122	0.42766	0.427657	0.49881	0.4988111
332	0	0	0	0	0	0	0	0

procedure. The results are presented in Tables 17 and 18 for ten different nodal points considering scaled arch dam models such as Model-1, Model-2, Model-3 and Model-4. It can be seen from these tables that there is a good agreement between finite element results and related formula.

For the principal stresses results, scale factor between prototype structure and scaled models is taken into consideration as  $\frac{1_m}{1_p} = \frac{1}{S}$ . In this paper, the terms of

prototype and model are used to emphasize the laboratory arch dam model and real constructed or under construction arch dam structures, respectively. So, Eq. (30) is rearranged as below to obtain the Eq. (41) using corresponding scale

factor  $\frac{1_m}{1_p} = S$ .

Considering the maximum principal stress values of prototype Type-1 arch dam given in Table 11 including dam-foundation interaction, the max principal stress value at 48th nodal point (middle of crest) of Model-1 and Model-2 are calculated using Eq. (41) as

$$\sigma_m = S \frac{\gamma_m}{\gamma_p} \sigma_p \quad (41)$$

For example, the max. principal stress value at 48th nodal point for Model-1 is obtained as

$$\left. \begin{aligned} \sigma_{m_1} &= S \frac{\lambda_{m_1}}{\gamma_p} \sigma_p \\ \sigma_{m_1} &= 335 \times \frac{2300}{2300} \times (-0.000142) = -0.04757 \text{ MPa} \end{aligned} \right\} (42)$$

For example, the max. principal stress value at 48th nodal point for Model-2 is obtained as

$$\left. \begin{aligned} \sigma_{m_2} &= S \frac{\lambda_{m_2}}{\gamma_p} \sigma_p \\ \sigma_{m_2} &= 400 \times \frac{2300}{2300} \times (-0.000142) = -0.0568 \text{ MPa} \end{aligned} \right\} (43)$$

All maximum and minimum principal stresses can be obtained using same procedure. The results are presented in Tables 19-22 for ten different nodal points considering scaled arch dam models such as Model-1, Model-2, Model-3 and Model-4. It can be seen from these tables that there is a good agreement between finite element results and related formula.

For the principal strain results, scale factor between prototype structure and scaled models is taken into

Table 19 The maximum principal stresses values of scaled arch dam models using FE analyses and formula for dam-foundation interaction

Nodal Points	Maximum Principal Stresses (MPa)							
	Model-1		Model-2		Model-3		Model-4	
	ANSYS	Formula	ANSYS	Formula	ANSYS	Formula	ANSYS	Formula
48	-0.04756	-0.04757	-0.05679	-0.0568	-0.05915	-0.05917	-0.06389	-0.06390
103	0.10258	0.102584	0.12249	0.122488	0.12759	0.12759	0.1378	0.13780
115	0.14257	0.142566	0.17023	0.170228	0.17732	0.17732	0.19151	0.19151
125	0.000887	0.000888	0.001059	0.00106	0.001103	0.00110	0.001191	0.00119
169	0.005034	0.005035	0.006011	0.006012	0.006262	0.00626	0.006762	0.00676
185	0.043147	0.043148	0.051519	0.05152	0.053666	0.05367	0.057958	0.05796
238	0.008146	0.009996	0.009727	0.011936	0.010132	0.01243	0.010943	0.01343
246	-0.00376	-0.00375	-0.00449	-0.00448	-0.00468	-0.00467	-0.00505	-0.00504
260	0.008366	0.008365	0.009989	0.009988	0.010405	0.01040	0.011238	0.01124
332	-0.45258	-0.45259	-0.5404	-0.5404	-0.56292	-0.56292	-0.60795	-0.60795

Table 20 The minimum principal stresses values of scaled arch dam models using FE analyses and formula for dam-foundation interaction

Nodal Points	Minimum Principal Stresses (MPa)							
	Model-1		Model-2		Model-3		Model-4	
	ANSYS	Formula	ANSYS	Formula	ANSYS	Formula	ANSYS	Formula
48	-0.39711	-0.39711	-0.47416	-0.47416	-0.49392	-0.49392	-0.53343	-0.53343
103	-1.3969	-1.39688	-1.6679	-1.66792	-1.7374	-1.73743	-1.8764	-1.87641
115	-1.3509	-1.35089	-1.613	-1.613	-1.6802	-1.68022	-1.8146	-1.81463
125	-1.3063	-1.3063	-1.5597	-1.55976	-1.6248	-1.62476	-1.7547	-1.75473
169	-1.9606	-1.96059	-2.341	-2.341	-2.4386	-2.43856	-2.6336	-2.63363
185	-1.7675	-1.76753	-2.1105	-2.11048	-2.1984	-2.19843	-2.3743	-2.37429
238	-2.6306	-2.9016	-3.1410	-3.4646	-3.2719	-3.60899	-3.5337	-3.89768
246	-2.8293	-2.82931	-3.3783	-3.37828	-3.5191	-3.51907	-3.8005	-3.80057
260	-2.5054	-2.50536	-2.9915	-2.99148	-3.1161	-3.11615	-3.3654	-3.36542
332	-2.857	-2.85698	-3.4113	-3.41132	-3.5535	-3.55349	-3.8377	-3.83774

Table 21 The maximum principal stresses values of scaled arch dam models using FE analyses and formula for fixed support condition

Nodal Points	Maximum Principal Stresses (MPa)							
	Model-1		Model-2		Model-3		Model-4	
	ANSYS	Formula	ANSYS	Formula	ANSYS	Formula	ANSYS	Formula
48	-0.05202	-0.05203	-0.06211	-0.06212	-0.0647	-0.06471	-0.06987	-0.06989
103	0.70214	0.70216	0.83838	0.8384	0.87332	0.87334	0.94318	0.9432
115	0.37151	0.371515	0.4436	0.4436	0.46209	0.46209	0.49905	0.49905
125	0.02101	0.021011	0.025087	0.025088	0.026132	0.02613	0.028223	0.02822
169	0.009072	0.009072	0.010832	0.010832	0.011283	0.01128	0.012186	0.01219
185	0.163500	0.163503	0.19523	0.195228	0.20336	0.20336	0.21963	0.21963
238	0.009562	0.009561	0.011418	0.011416	0.011894	0.01189	0.012845	0.01284
246	-0.00542	-0.00543	-0.00647	-0.00648	-0.00674	-0.00675	-0.00727	-0.00729
260	0.0080635	0.008063	0.096281	0.009628	0.010029	0.01003	0.010832	0.01083
332	-0.7499	-0.7499	-0.8954	-0.8954	-0.93272	-0.93272	-1.0073	-1.00733

consideration as  $\frac{1_m}{1_p} = \frac{1}{S}$ . In this paper, the terms of

prototype and model are used to emphasize the laboratory arch dam model and real constructed or under construction arch dam structures, respectively. So, Eq. (35) is rearranged as below to obtain the Eq. (44) using corresponding scale

$$\text{factor } \frac{1_m}{1_p} = S.$$

Considering the maximum principal strain values of prototype Type-1 arch dam given in Table 12 including dam-foundation interaction, the max principal strain value at 48th nodal point (middle of crest) of Model-1 and Model-

Table 22 The minimum principal stresses values of scaled arch dam models using FE analyses and formula for fixed support condition

Nodal Points	Minimum Principal Stresses (MPa)							
	Model-1		Model-2		Model-3		Model-4	
	ANSYS	Formula	ANSYS	Formula	ANSYS	Formula	ANSYS	Formula
48	-1.0892	-1.08925	-1.3006	-1.3006	-1.3548	-1.3548	-1.4632	-1.46318
103	-1.4299	-1.42991	-1.7074	-1.70736	-1.7785	-1.77851	-1.9208	-1.92078
115	-1.1651	-1.16513	-1.3912	-1.3912	-1.4492	-1.44918	-1.5651	-1.5651
125	-1.5532	-1.55323	-1.8546	-1.8546	-1.9319	-1.93189	-2.0864	-2.08643
169	-1.8378	-1.83784	-2.1944	-2.19444	-2.2859	-2.28589	-2.4687	-2.46875
185	-1.6636	-1.66364	-1.9864	-1.98644	-2.0692	-2.06922	-2.2347	-2.23475
238	-2.4035	-2.40349	-2.8698	-2.86984	-2.9894	-2.98944	-3.2286	-3.22857
246	-2.5219	-2.52191	-3.0112	-3.01124	-3.1367	-3.13673	-3.3876	-3.38765
260	-2.4657	-2.4657	-2.9441	-2.94412	-3.0668	-3.06682	-3.3121	-3.31214
332	-2.8629	-2.86288	-3.4184	-3.41836	-3.5608	-3.56082	-3.8457	-3.84566

Table 23 The maximum principal strain values of scaled arch dam models using FE analyses and formula for dam-foundation interaction

Nodal Points	Maximum Principal Strains							
	Model-1		Model-2		Model-3		Model-4	
	ANSYS	Formula	ANSYS	Formula	ANSYS	Formula	ANSYS	Formula
48	2.288E-06	2.288E-6	2.733E-06	2.733E-6	2.846E-6	2.846E-6	3.074E-6	3.074E-6
103	1.121E-05	1.121E-5	1.338E-05	1.338E-5	1.394E-5	1.394E-5	1.505E-5	1.505E-5
115	1.214E-05	1.214E-5	1.450E-05	1.450E-5	1.510E-5	1.510E-5	1.631E-5	1.631E-5
125	7.899E-06	7.899E-6	9.432E-06	9.432E-6	9.825E-6	9.825E-6	1.061E-5	1.061E-5
169	1.269E-05	1.269E-5	1.515E-05	1.515E-5	1.578E-5	1.578E-5	1.704E-5	1.704E-5
185	1.164E-05	1.164E-5	1.390E-05	1.390E-5	1.448E-5	1.448E-5	1.564E-5	1.564E-5
238	1.691E-05	1.691E-5	2.019E-05	2.019E-5	2.103E-5	2.103E-5	2.271E-5	2.271E-5
246	1.829E-05	1.829E-5	2.183E-05	2.183E-5	2.274E-5	2.274E-5	2.456E-5	2.456E-5
260	1.574E-05	1.575E-5	1.880E-05	1.880E-5	1.958E-5	1.958E-5	2.115E-5	2.115E-5
332	9.062E-06	9.062E-6	1.082E-05	1.082E-5	1.127E-5	1.127E-5	1.217E-5	1.217E-5

Table 24 The minimum principal strain values of scaled arch dam models using FE analyses and formula for dam-foundation interaction

Nodal Points	Minimum Principal Strains							
	Model-1		Model-2		Model-3		Model-4	
	ANSYS	Formula	ANSYS	Formula	ANSYS	Formula	ANSYS	Formula
48	-1.005E-5	-1.005E-5	-1.200E-05	-1.200E-5	-1.250E-5	-1.250E-5	-1.350E-5	-1.350E-5
103	-4.172E-5	-4.172E-5	-4.981E-05	-4.981E-5	-5.189E-5	-5.189E-5	-5.604E-5	-5.604E-5
115	-4.057E-5	-4.057E-5	-4.844E-05	-4.844E-5	-5.046E-5	-5.046E-5	-5.449E-5	-5.449E-5
125	-3.824E-5	-3.824E-5	-4.566E-05	-4.566E-5	-4.756E-5	-4.756E-5	-5.136E-5	-5.136E-5
169	-5.669E-5	-5.669E-5	-6.769E-05	-6.769E-5	-7.051E-5	-7.051E-5	-7.615E-5	-7.615E-5
185	-5.227E-5	-5.227E-5	-6.241E-05	-6.241E-5	-6.501E-5	-6.501E-5	-7.021E-5	-7.021E-5
238	-7.623E-5	-7.622E-5	-9.102E-05	-9.102E-5	-9.481E-5	-9.481E-5	-1.024E-4	-1.024E-4
246	-8.144E-5	-8.144E-5	-9.724E-05	-9.724E-5	-1.013E-4	-1.013E-4	-1.094E-4	-1.094E-4
260	-7.298E-5	-7.297E-5	-8.713E-05	-8.713E-5	-9.077E-5	-9.077E-5	-9.803E-5	-9.803E-5
332	-7.580E-5	-7.579E-5	-9.051E-05	-9.049E-5	-9.428E-5	-9.427E-5	-1.018E-4	-1.018E-4

2 are calculated using Eq. (41) as

$$\varepsilon_m = S \frac{\gamma_p E_p}{\gamma_m E_m} \varepsilon_p \quad (44)$$

For example, the max. principal strain value at 48th nodal point for Model-1 is obtained as

$$\varepsilon_m = S \frac{\gamma_p E_p}{\gamma_m E_m} \varepsilon_p \quad (45)$$

$$\varepsilon_m = 333 \frac{2300 \ 15000}{2300 \ 34000} - 1.5484 E - 8 = 2.2884 E - 6$$

For example, the max. principal strain value at 48th

Table 25 The maximum principal strain values of scaled arch dam models using FE analyses and formula for fixed support condition

Nodal Points	Maximum Principal Strains							
	Model-1		Model-2		Model-3		Model-4	
	ANSYS	Formula	ANSYS	Formula	ANSYS	Formula	ANSYS	Formula
48	7.345E-6	7.345E-6	8.770E-6	8.770E-6	9.135E-6	9.135E-6	9.866E-6	9.866E-6
103	2.893E-5	2.893E-5	3.454E-5	3.454E-5	3.598E-5	3.598E-5	3.886E-5	3.886E-5
115	1.780E-5	1.780E-5	2.125E-5	2.125E-5	2.214E-5	2.214E-5	2.391E-5	2.391E-5
125	9.832E-6	9.832E-6	1.174E-5	1.174E-5	1.223E-5	1.223E-5	1.321E-5	1.321E-5
169	1.295E-5	1.295E-5	1.547E-5	1.547E-5	1.611E-5	1.611E-5	1.740E-5	1.740E-5
185	1.457E-5	1.457E-5	1.740E-5	1.740E-5	1.813E-5	1.813E-5	1.958E-5	1.958E-5
238	1.520E-5	1.520E-5	1.815E-5	1.815E-5	1.891E-5	1.891E-5	2.042E-5	2.042E-5
246	1.847E-5	1.846E-5	2.205E-5	2.205E-5	2.297E-5	2.297E-5	2.480E-5	2.480E-5
260	1.546E-5	1.546E-5	1.846E-5	1.846E-5	1.923E-5	1.923E-5	2.076E-5	2.076E-5
332	3.876E-5	3.876E-5	4.628E-5	4.628E-5	4.436E-7	4.436E-7	4.791E-7	4.791E-7

Table 26 The minimum principal strain values of scaled arch dam models using FE analyses and formula for fixed support condition

Nodal Points	Minimum Principal Strains							
	Model-1		Model-2		Model-3		Model-4	
	ANSYS	Formula	ANSYS	Formula	ANSYS	Formula	ANSYS	Formula
48	-2.926E-5	-2.926E-5	-3.494E-5	-3.494E-5	-3.640E-5	-3.640E-5	-3.931E-5	-3.931E-5
103	-4.632E-5	-4.871E-5	-5.531E-5	-5.817E-5	-5.761E-5	-6.059E-5	-6.222E-5	-6.544E-5
115	-3.644E-5	-3.899E-5	-4.351E-5	-4.655E-5	-4.532E-5	-4.849E-5	-4.894E-5	-5.237E-5
125	-4.573E-5	-4.573E-5	-5.460E-5	-5.460E-5	-5.688E-5	-5.688E-5	-6.143E-5	-6.143E-5
169	-5.223E-5	-5.223E-5	-6.237E-5	-6.237E-5	-6.497E-5	-6.497E-5	-7.016E-5	-7.016E-5
185	-4.991E-5	-4.991E-5	-5.960E-5	-5.960E-5	-6.208E-5	-6.208E-5	-6.705E-5	-6.705E-5
238	-6.996E-5	-6.996E-5	-8.354E-5	-8.354E-5	-8.702E-5	-8.702E-5	-9.398E-5	-9.398E-5
246	-7.035E-5	-7.035E-5	-8.400E-5	-8.400E-5	-8.750E-5	-8.750E-5	-9.450E-5	-9.450E-5
260	-7.185E-5	-7.185E-5	-8.579E-5	-8.579E-5	-8.937E-5	-8.937E-5	-9.652E-5	-9.652E-5
332	-7.422E-5	-7.422E-5	-8.862E-5	-8.862E-5	-9.231E-5	-9.231E-5	-9.970E-5	-9.970E-5

nodal point for Model-2 is obtained as

$$\left. \begin{aligned} \varepsilon_{m_2} &= S \frac{\gamma_p}{\gamma_{m_2}} \frac{E_p}{E_{m_2}} \varepsilon_p \\ \varepsilon_{m_2} &= 400 \frac{2300}{2300} \frac{15000}{34000} 1.5484 E - 8 = 2.7325 E - 6 \end{aligned} \right\} (46)$$

All maximum and minimum principal strains can be obtained using same procedure. The results are presented in Tables 23-26 for ten different nodal points considering scaled arch dam models such as Model-1, Model-2, Model-3 and Model-4. It can be seen from these tables that there is a good agreement between finite element results and related formula.

## 5. Conclusions

This paper presents the determination of dynamic characteristics and internal forces of arch dams considering experimentally validated prototype laboratory model using similitude and scaling laws. Type-1 arch dam, which is one of five arch dam types suggested at the ‘‘Arch Dams’’ Symposium in England in 1968 is selected as reference prototype model and the analysis are performed both dam-

foundation interaction and fixed support condition. The following observations can be made from the study:

The structural behavior of laboratory arch dam (prototype model) is determined using numerical and experimental methods to use the results as reference parameters for scaling. From the results, it is seen that finite element model and analyses of the prototype Type-1 arch dam can be safely used to predict the structural response of arch dams with different dimensions and material properties.

To investigate the real arch dam response using scaling laws and similarity requirements with related formulas, four different arch dam (Berke arch dam as Model-1, Sayano arch dam as Model-2, Deriner arch dam as Model-3, and Yusufeli arch dam as Model-4) are selected as an example with 201m, 240m, 250m and 270m arch heights considering 335, 400, 416.67 and 450 scale factors, respectively.

The natural frequencies, displacements, maximum-minimum principal stresses and strains are calculated and presented with comparison for each arch dam model by using similitude formulas.

At the end of the study, it is seen that there is a good agreement between all results (dynamic characteristics and internal forces) obtained by similarity requirements with scaling laws and enlarged finite element models. The

differences are calculated as nearly 0%.

## References

- Altunışık, A.C., Günaydın, M., Sevim, B. and Adanur, S. (2017), "System identification of arch dam model strengthened with cfrp composite materials", *Steel Compos. Struct.*, **25**(2), 231-244.
- Altunışık, A.C., Günaydın, M., Sevim, B. and Bayraktar, A. (2016), "Retrofitting effect on the dynamic properties of model-arch dam with and without reservoir water using ambient-vibration test methods", *J. Struct. Eng.*, **142**(10), 04016069.
- Altunışık, A.C., Günaydın, M., Sevim, B., Bayraktar, A. and Adanur, S. (2015), "CFRP composite retrofitting effect on the dynamic characteristics of arch dams", *Soil Dyn. Earthq. Eng.*, **74**, 1-9.
- Altunışık, A.C., Karahasan, O.Ş., Genç, A.F., Okur, F.Y., Günaydın, M., Kalkan, E. and Adanur, S. (2018), "Modal parameter identification of RC frame under undamaged, damaged, repaired and strengthened conditions", *Measurement*, **124**, 260-276.
- ANSYS (2016), Swanson Analysis System, USA.
- Arch Dams (1968), "A review of British research and development", *Proceedings of the Symposium held at the Institution of Civil Engineers*, March, London, England.
- Balaguer, P. and Claramonte, J.A. (2011), "Characterization and control of dimensionally similar systems", *J. Franklin Inst.*, **348**, 1814-1831.
- Balawi, S., Shahid, O. and Mulla, M.A. (2015), "Similitude and scaling laws-static and dynamic behaviour beams and plates", *Procedia Eng.*, **114**, 330-337.
- Başbolat, E.E., Bayraktar, A., Başağa, H.B. and Türker, T. (2013), "Determination of experimental dynamic characteristics of Deriner Concrete Arch Dam", *Turkey Earthquake Engineering and Seismology Conference*, September, Hatay, Turkey. (in Turkish)
- Carpinteri, A. and Corrado, M. (2010), "Dimensional analysis approach to the plastic rotation capacity of over-reinforced concrete beams", *Eng. Fract. Mech.*, **77**, 1091-1100.
- Chen, X., Wu, S. and Zhou, J. (2015), "Large-beam tests on mechanical behavior of dam concrete under dynamic loading", *J. Mater. Civil Eng.*, **27**(10), 06015001.
- Chen, Z., Chen, W., Li, Y. and Yuan, Y. (2016), "Shaking table test of a multi-story subway station under pulse-like ground motions", *Soil Dyn. Earthq. Eng.*, **82**, 111-122.
- Chen, Z.Y. and Shen, H. (2014), "Dynamic centrifuge tests on isolation mechanism of tunnels subjected to seismic shaking", *Tunnel. Underg. Space Technol.*, **42**, 67-77.
- Datin, P.L. and Prevatt, D.O. (2013), "Using instrumented small-scale models to study structural load paths in wood-framed buildings", *Eng. Struct.*, **54**, 47-56.
- Ghosh, A. (2011), "Scaling laws", *Mechanics Over Micro and Nano Scales*, Springer, New York, NY.
- Hafeez, F. and Almaskari, F. (2015), "Experimental investigation of the scaling laws in laterally indented filament wound tubes supported with v shaped cradles", *Compos. Struct.*, **126**, 265-284.
- Huang, Y. and Zhu, C.Q. (2017), "Safety assessment of antiliquefaction performance of a constructed reservoir embankment. I: Experimental assessment", *J. Perform. Constr. Facil.*, **31**(2), 04016101.
- Jiang, D. and Shu, D. (2005), "Prediction of peak acceleration of one degree of freedom structures by scaling law", *J. Struct. Eng.*, **131**(4), 582-588.
- Kalateh, F. and Koosheh, A. (2017), "Comparing of loose and strong finite element partitioned coupling methods of acoustic fluid-structure interaction: concrete dam-reservoir system", *KSCE J. Civil Eng.*, **21**(3), 807-817.
- Khiavi, M.P. (2017), "Investigation of seismic performance of concrete gravity dams using probabilistic analysis", *Croatian Soc. Civil, Hsgi, Gradevinar*, **69**(1), 21-29.
- Lokke, A. and Chopra, A.K. (2017), "Direct finite element method for nonlinear analysis of semi-unbounded dam-water-foundation rock systems", *Earthq. Eng. Struct. Dyn.*, **46**(8), 1267-1285..
- Lu, X., Zhou, B. and Lu, W. (2015), "Shaking table test and numerical analysis of a high-rise building with steel reinforce concrete column and reinforce concrete core tube", *Struct. Des. Tall Spec. Build.*, **24**, 1019-1038.
- Luo, D., Hu, Y. and Li, Q. (2016), "An interfacial layer element for finite element analysis of arch dams", *Eng. Struct.*, **128**, 400-414.
- Oliveira, S. and Faria, R. (2006), "Numerical simulation of collapse scenarios in reduced scale tests of arch dams", *Eng. Struct.*, **28**, 1430-1439.
- Prabhu, Raja, V., Ramu, M. and Thyła, P.R. (2013), "Analytical and numerical validation of the developed structural similitude for elastic models", *Ind. J. Eng. Mater. Sci.*, **20**, 492-496.
- Ramu, M., Prabhu, Raja, V. and Thyła, P.R. (2013), "Establishment of structural similitude for elastic models and validation of scaling laws", *KSCE J. Civil Eng.*, **17**(1), 139-144.
- Sevim, B. (2010), "Determination of dynamic behavior of arch dams using finite element and experimental modal analysis methods", Ph.D. Dissertation, Karadeniz Technical University, Trabzon, Turkey.
- Sevim, B., Altunışık, A.C. and Bayraktar, A. (2012), "Experimental evaluation of crack effects on the dynamic characteristics of a prototype arch dam using ambient vibration tests", *Comput. Concrete*, **10**(3), 277-294.
- Sevim, B., Altunışık, A.C. and Bayraktar, A. (2013), "Structural identification of concrete arch dams by ambient vibration tests", *Adv. Concrete Constr.*, **1**(3), 227-237.
- Sevim, B., Altunışık, A.C. and Bayraktar, A. (2014), "Construction stages analyses using time dependent material properties of concrete arch dams", *Comput. Concrete*, **14**(5), 599-612.
- Sevim, B., Bayraktar, A. and Altunışık, A.C. (2009), "Finite element model calibration of Berke Arch Dam using operational modal testing", *J. Vib. Control*, **17**(7), 1065-1079.
- Sevim, B., Bayraktar, A. and Altunışık, A.C. (2011), "Investigation of water length effects on the modal behavior of a prototype arch dam using operational and analytical modal analyses", *Struct. Eng. Mech.*, **37**(6), 593-615.
- Shehadeh, M., Shennawy, Y. and El-Gamal, H. (2015), "Similitude and scaling of large structural elements: case study", *Alexandria Eng. J.*, **54**, 147-154.
- URL-1. 15http://eng.harran.edu.tr/moodle/moodledata/7/yesilata/01\_Ders\_Notlari/07ch4.pdf, 26.06.2017.
- Wang, B.S. and He, Z.C. (2007), "Crack detection of arch dam using statistical neural network based on the reductions of natural frequencies", *J. Sound Vib.*, **302**, 1037-1047.
- Wang, H. and Li, D. (2006), "Experimental study of seismic overloading of large arch dam", *Earthq. Eng. Struct. Dyn.*, **35**, 199-216.
- Wang, H. and Li, D. (2007), "Experimental study of dynamic damage of an arch dam", *Earthq. Eng. Struct. Dyn.*, **36**, 347-366.
- Wang, H., Wang, L., Song, Y. and Wang, J. (2016), "Influence of free water on dynamic behavior of dam concrete under biaxial compression", *Constr. Build. Mater.*, **112**, 222-231.
- Zhongzhi, F., Shengshui, C. and Huaqiang, H. (2017), "Experimental investigations on the residual strain behavior of a rockfill material subjected to dynamic loading", *J. Mater. Civil*

*Eng.*, **29**(5), 04016278.

Zhou, J., Lin, G., Zhu, T., Jefferson, A.D. and Williams, F.W.  
(2000), "Experimental investigation into seismic failure of high  
arch dams", *J. Struct. Eng.*, ASCE, **126**, 926-935.

CC